

Preparation of Fe-Co-Ni Ternary Alloys with Electrodeposition

Yufang Yang

Department of Chemistry, Hanshan Normal University, Chaozhou 521041, China

*E-mail: zzyufang@163.com

Received: 13 October 2014 / Accepted: 14 April 2015 / Published: 28 April 2015

Electrodeposition of Fe-Co-Ni ternary alloys was performed in a chloride-sulphate-tartaric acid medium. The influences of electroplating parameters such as current density, temperature, pH value and electrolyte composition on depositing rate, compositions of Fe-Co-Ni deposits and electrodeposition behavior on titanium substrate were investigated. The composition, morphology and the microstructure of deposits were analyzed by EDS, SEM and XRD, respectively. The results indicated that the optimum conditions for obtaining Co-rich Fe-Co-Ni alloys were current density of 4 A/dm², temperature of 40 °C, pH of 2.3-3.2, tartaric acid concentration of 8-12 g/l, Co^{2+}/Ni^{2+} molar ratio of 0.26-0.4. The codeposition of Fe-Co-Ni alloy is anomalous; namely Fe is more easily deposited than Co, and Co is easily deposited than Ni. However, the deposition order of Fe and Co is affected by temperature and Co^{2+}/Ni^{2+} ratio. The Fe-Co-Ni ternary alloys with 15.62-20.56% of Fe, 43.84-61.93% of Co, 22.45%-40.05% of Ni were bright and super toughness with low residual stress. The SEM showed that fine-grain, smooth and compact Fe-Co-Ni alloy deposits were obtained. The crystallographic structure of the deposit was the bcc solid solution.

Keywords: Electrodeposition; Iron-Cobalt-Nickel; Ternary alloys

1. INTRODUCTION

Fe-Co-Ni alloy is an important transition metal alloy which attracted many people's attention because of its outstanding magnetism performance, super physical and chemical properties [1-3]. For example, the saturated magnetic flux and the electronic resistance of rich cobalt alloy Co₇₃Ni₁₅Fe₁₂ are higher than that of permalloy Ni₈₀Fe₂₀ by far, which can be served as the magnetic head in the super high density magnetic recording [4]. The rich iron alloy of Fe₆₄Co₅Ni₃₁ has a low thermal expansion coefficient, which can be available in precise microwave conduit, astronavigation lens, laser box, printed circuit board and so on. Fe-Co-Ni alloy can be prepared by many ways, for example mechanical alloying [5], DC arc plasma [6], template [7], electrodeposition. As electrodeposition of

Fe-Co-Ni is usually much cheaper and simpler than the other methods, it attracts researchers' consideration [8-14]. The Fe-Co-Ni ternary alloy prepared by electrodeposition has high saturation induction density (B_s), low coercive force (H_c). Its hardness, corrosion resistance and superficial radiance are close to that of the hard chromium deposit. It may replace the actual widely used hard chromium plating in certain degree [3]. The magnetism performance of Fe-Co-Ni ternary is relative to its thickness and composition. When the Co content exceeds 65%, the deposit layer is nearly the zero magnetostriction. Ni-Fe-Co alloy nanowires can be electrodeposited in modified anodic aluminum oxide (AAO) template [7] or by using cyclic voltammetry and pulse-reverse electroplating [15-16]. However, literatures related to Fe-Co-Ni alloy film electrodeposition are fewer. In this paper, influences of current density, temperature, pH value and electrolyte component on the deposition rate, compositions of the deposit and the deposition characteristics of Fe-Co-Ni alloy are investigated in detailed. The novelty of this work is to prepare the excellent performance rich cobalt Fe-Co-Ni ternary alloy materials which can be completely peeled off from the substrate.

2. EXPERIMENTAL

All Fe-Co- Ni alloys were electrodeposited on one side of $4 \times 2.5 \times 0.1$ cm samples made of titanium sheet. The advantage of using titanium as cathode is that it is convenient to easily peel off the Fe-Co- Ni ternary from the substrate. The substrates were polished mechanically with silicon carbide emery paper. Prior to deposition, the substrates were rinsed in flowing water and degreased in acetone, dipped in the mixed solution of 10wt% HNO_3 and 10wt% HF for activation for 30s and then washed thoroughly in deionized water.

Fe-Co- Ni alloys were electrodeposited from a solution containing 0.304 M of $NiSO_4 \cdot 6H_2O$, 0.084 M of $NiCl_2 \cdot 6H_2O$, 0.1 M of $CoSO_4 \cdot 7H_2O$, 0.036 M of $FeSO_4 \cdot 7H_2O$, 20 g/l of H_3BO_3 , 2 g/l of stabilizer, 4 g/l of tartaric acid, 4 g/l of brightener and 0.1 g/l of wetting agent. The solution was freshly prepared in deionized water using analytical grade reagent.

The electrodeposition was carried out in a 300ml rectangular PVC cell with an agitator at current densities of 2-6 A/dm^2 . The temperature of the electrolytes was varied from 30 °C to 70 °C and the pH value was in the range from 1.4 to 5.2. The deposition time was 15min. The pH value of the bath was adjusted with the diluted hydrochloric acid and sodium hydroxide solution.

Electrolytic nickel was used as an anode. The area ratio of anode to cathode was kept at 2. The distance between the two electrodes was 5cm. After plating, the deposited films were thoroughly washed with distilled water, peeled off from the substrate, dried with hot air and weighed.

The composition of each deposited film was determined by means of an EDX-GENESIS 60S (EDAXInC,USA) energy dispersive spectrometer (EDS). The morphologies of Fe-Co- Ni ternary alloys were examined by a JSM-6360LV scanning electron microscope (SEM). The structure of Fe-Co- Ni alloy was investigated by X-ray diffraction (XRD) (Rigaku D/max 2500) at 40kv and 250mA using Ni filter and Cu α -radiation. The scan region (2θ) was ranged from 30° to 100° at a scan rate of 0.02°/s.

The cathodic polarization curves were performed by electrochemical workstation, CHI 660C. The working electrode was a copper wire with a diameter of 1mm. The counter electrode was a platinum foil with an area of 4 cm² and a saturated calomel electrode (SCE) was used as a reference. The polarization curves were carried out at a 1 mV/s scan rate.

3.RESULTS AND DISCUSSION

3.1. Influence of current density on Fe-Co- Ni alloy deposition

Fig. 1 shows the influence of current density on Fe-Co-Ni alloy codeposition at temperature of 40 °C and at pH of 2.3.

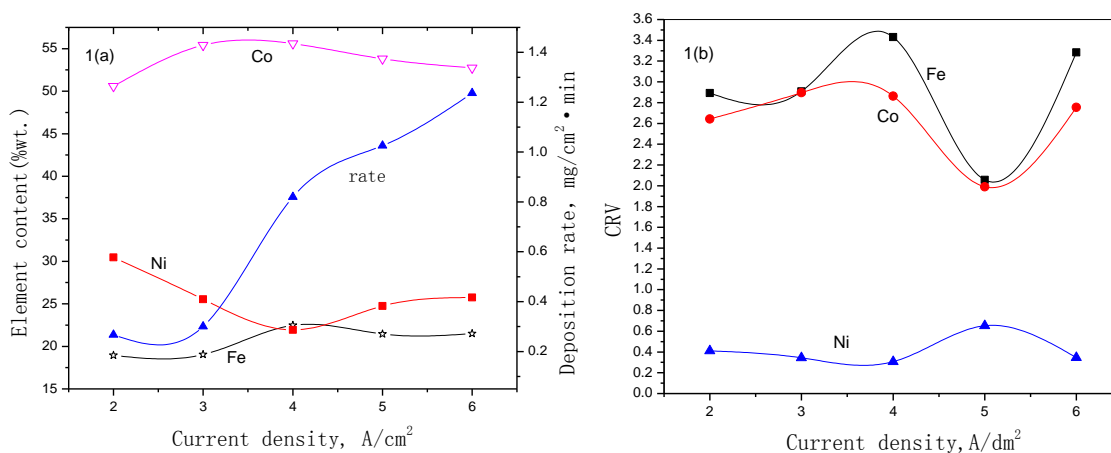


Figure 1. Influence of current density on Fe-Co-Ni alloy electrodeposition

As shown in Fig.1 (a), the deposition rate of Fe-Co-Ni alloy increased gradually with the increase of current density. When the current density was 2-3 A/dm², the deposition rate increased slowly and increased quickly when the current density was 3-6 A/dm², rising from 0.3 mg/cm²·min to 1.24 mg/cm²·min. Higher current density is beneficial to the deposition rate. However, the higher the current density, the faster the hydrogen evolution reaction is, leading to the decrease of current efficiency.

With the increase of current density, the content of Fe and Co in the deposits first increased and then reached the maximum at 4 A/dm². With a further increase in the current density, the weight percentage of Fe and Co decreased gradually. However, the content of Ni in the deposits first decreased and then increased, reaching to a minimum at 4 A/dm². All the deposits were Co rich across the current density range from 2 to 6 A/dm². In the range of 2-4 A/dm², the increase of current density is advantageous to the electrodeposition of Fe and Co, but does not favour the deposition of Ni. When the current density is greater than 4 A/dm², the deposition rate of Fe and Co is accelerated. Therefore the concentration polarization appears near the electrode surface, leading to a decrease in Fe and Co content in the deposit and the increase in Ni content.

The experiments indicated that the deposit obtained at current density less than 3 A/dm² was dull with a big residual stress and easy to crack. When the current density was in the range of 3-5 A/dm², the obtained deposit was bright and smooth. When the current density was greater than 5 A/dm², the edge of the deposit was burnt to black and the bright area of the deposit narrowed visibly. The current density of 4 A/dm² is appropriate, at which the deposit with bright and smooth surface and good toughness can be obtained. The weight percentage of Fe, Co and Ni in the obtained deposit is 22.47%, 55.6% and 21.94%, respectively.

It is known that the content of Fe, Co and Ni in the electrolyte is 6.55%, 19.13% and 74.32%, respectively. It can be seen from Fig.1 (a) that the contents of Fe and Co in the deposits are greater than the concentration of Fe and Co in the electrolyte by far, whereas the content of Ni is lower in the deposit than in the electrolyte. In Fig.1 (b), the ordinate is the composition ratio value (CRV) defined as:

$$CRV = \frac{Fe(Co, Ni)\%wt. \text{ in deposit}}{Fe(Co, Ni)\%wt. \text{ in electrolyte}}$$

Where numerator is weight percent of Fe (or Co, Ni) in the deposit, denominator is weight percent of Fe (or Co, Ni) in the electrolyte.

Fig.1(b) indicates that Fe content in the deposits is 2.06-3.43 times Fe content in the electrolyte, Co content in the deposits is 1.99-2.9 times Co content in the electrolyte, and Ni content in the deposits is 0.34-0.65 times Ni content in the electrolyte. The curve of Co is located under the curve of Fe but is located above the curve of Ni, explaining that in the process of codeposition the deposition rate of the more negative Fe and Co is speeded up, while the deposition rate of the more positive Ni is slowed down. Fe deposits prior to Co and Co deposits prior to Ni. The electrodeposition of Fe-Co-Ni alloy is an anomalous codeposition. This anomalous deposition is in agreement with the definition defined by Brenner [17]. The anomalous deposition was attributed to hydrogen evolution at the cathode surface. The hydrogen evolution depleted protons and resulted in increasing the local concentration of hydroxyl ions [18], which led to the formation and adsorption of metal hydroxide ions on cathode surface, favoring the anomalous deposition of Fe-Co-Ni alloy. It can be seen from Fig.1(b) that with increase of current density, the anomalous codeposition characteristics remains unchanged.

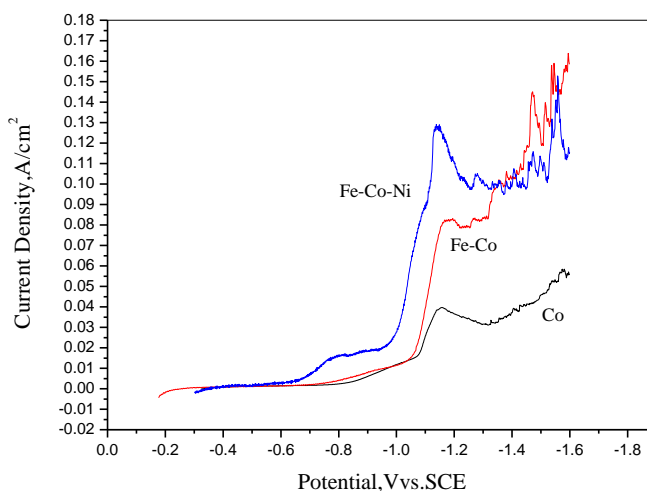


Figure 2. Polarization curves for Co, Fe-Co and Fe-Co –Ni electrodeposition at scanning rate of 1mV/s

Fig.2 illustrates the relationship between the current density and the cathodic potential for different electrolytes, i.e. 0.1M Co²⁺, 0.036 M Fe²⁺-0.1 M Co²⁺, and 0.036 M Fe²⁺-0.1 M Co²⁺- 0.084M Ni²⁺, operating at 40°C and pH of 2. The electrodeposition for electrolyte containing 0.1M Co²⁺ begins at around -0.80V. The current density increases slowly below -0.80V and keeps on till -1.075V where the current density abruptly increases and reaches the maximum at -1.155V. For the 0.036 M Fe²⁺-0.1 M Co²⁺ electrolyte, electrodeposition starts at -0.755V and gradually increases until to -1.05V where the current density quickly increases to the highest point at -1.17V. With addition of Ni²⁺ to the Fe²⁺-Co²⁺ solution, the curve of Fe-Co-Ni codeposition is shifted to the more positive potential. It shows that the polarization curve of Fe- Ni–Co codeposition resembles that of Fe-Co codeposition. As the potential increases cathodically from -0.65V, Fe-Co-Ni alloy begins to deposit. At the potential of -0.765V to -0.964V, the current density reaches the limiting stage. Then current density abruptly increases and reaches the maximum at -1.15V. When the potential continues to increase negatively, the Fe- Ni–Co codeposition suffers serious inhibition, as shown by the drop in current density, indicating the thickness of the diffusion layer increases and the precipitation of metal hydroxide on the cathode surface occurs. It can also be seen from Fig.2 that the rate of Fe- Ni–Co codeposition is larger than that of Fe- Co, indicating that Ni²⁺ promotes the deposition of Fe and Co. It also can be seen that the trend of the curve for Fe-Ni-Co codeposition is in agreement with observations for anomalous codeposition presented in literature [19,20].

3.2. Influence of temperature on Fe-Co- Ni alloy deposition

Fig.3. shows the influence of temperature on Fe-Co- Ni alloy codeposition at current density of 3 A/dm² and at pH of 2.3.

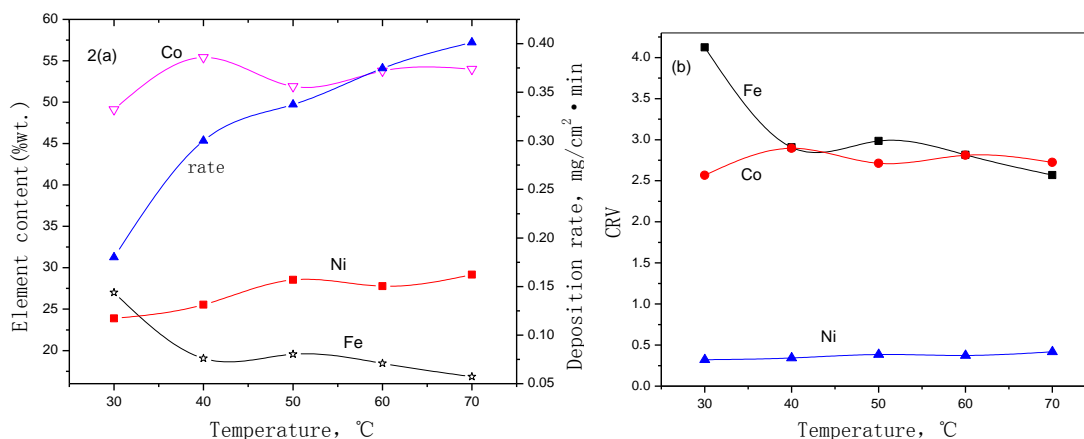


Figure 3. Influence of temperature on Fe-Co-Ni alloy electrodeposition

Fig.3(a) indicates that the Fe-Co-Ni alloy deposition rate increases with the increase of temperature. Due to the high temperature, the diffusive speed of the metallic ions in the electrolyte accelerate, which causes the increase of concentration of metallic ions in the cathode diffusion layer and favours the decrease of the cathodic polarization, leading the depositing rate to quicken. When the temperature was lower than 30 °C, the deposition rate was slow and the obtained deposit was thin. The surface of the deposit was black and coarse with a poor brightness.

With increase of temperature, the Fe content in the deposits decreased. It is well-known [21] that part of Fe²⁺ may oxidize to Fe³⁺ and form Fe (OH)₃, which is insoluble and precipitates at the bottom of the bath. With the increase of temperature, the oxidation rate of Fe²⁺ ions speeds. Therefore, Fe²⁺ concentration in the electrolyte reduces, leading to a decrease in Fe content in the deposits. The content of Co and Ni in the deposits increases first and then decreases, but the variable amount of Ni content is smaller. At temperature of 40 °C, the bright and smooth Fe-Co-Ni alloy deposit with good toughness can be obtained, and the compositions of the deposit is 19.04% Fe, 55.42% Co and 25.53% Ni, respectively. When the temperature was higher than 50 °C, the stability of the electrolyte decreased. At the same time, the compactness of the deposit was bad, its brightness and toughness got worse. Therefore, the more appropriate temperature was 40 °C.

It can be seen from Fig.3(b) that the Fe content in the deposits is 2.57-4.12 times the content of Fe in the electrolyte, the Co content in the deposits is 2.57-2.9 times the Co content in the electrolyte, and the Ni content in the deposits is 0.32-0.42 times the Ni content in the electrolyte; this shows that Fe and Co deposit are more preferred than Ni deposits. When the temperature is lower than 60 °C, the increase multiple of Fe in the deposit is larger than that of Co, indicating that Fe deposits preferentially than Co does. However, when temperature is higher than 60 °C, a transition from anomalous to normal deposition occurs, indicating that Co deposits preferentially than Fe deposits.

3.3. Influence of pH value on Fe-Co- Ni alloy deposition

Fig.4 shows the influence of pH value on Fe-Co-Ni alloy deposition at 3 A/dm² and 40 °C.

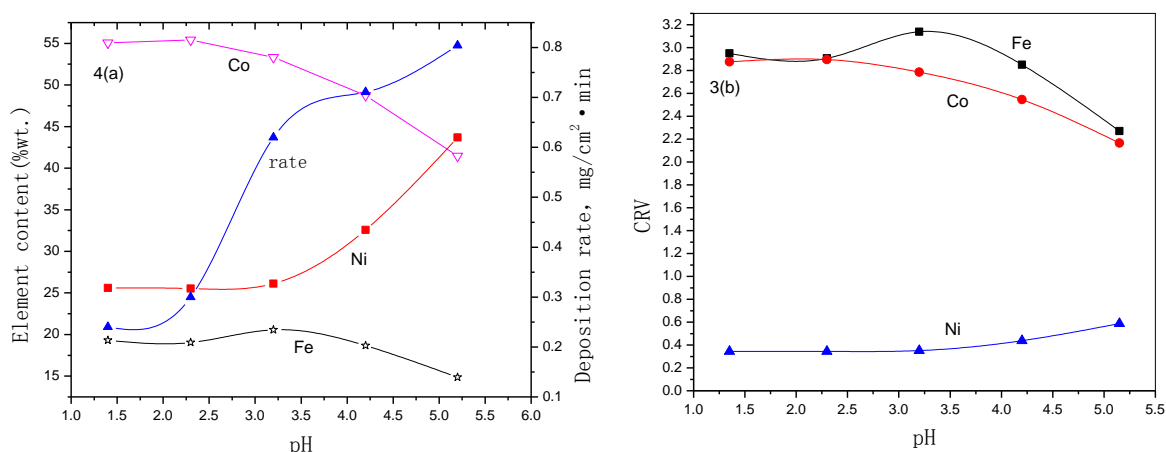


Figure 4. Influence of pH on Fe-Co-Ni alloy electrodeposition

Fig.4(a) indicates that the deposition rate increases with the increase of pH value; especially, when pH value increases from 2.3 to 3.2, the deposition rate increases quickly, rising from 0.3 mg/cm²·min to 0.62 mg/cm²·min. When the pH value was greater than 3.2, the deposition rate increased slowly. This is mainly due to the rise of pH value, resulting in the rate of hydrogen evolution to slow down, hence promoting the Fe-Co-Ni alloy codeposition.

When the pH value is in the range of 1.4 to 3.2, the content of Fe, Co and Ni in the deposit remains almost invariant. When the pH value is higher than 3.2, Fe and Co content in the deposits decreases gradually with the increase of pH value, while Ni content increases. Experiments showed that when the pH value was less than 2.3, the cathodic hydrogen evolution reaction was fierce; pinholes and burrs were found on the surface of the deposit, and the deposit was thin and brittle. When the pH value was 2.3 - 3.2, the hydrogen evolution reaction slowed, the deposit was smooth and bright with good toughness. When the pH value was greater than 3.2, the quality of the deposit became increasingly worse. Especially when the pH value was greater than 4, the toughness of the deposit decreased, charred and black phenomenon appeared on the edge of the coating, which may be caused by the fact that the higher pH value in the electrolyte is easy to form a metallic hydroxide precipitation. So the more appropriate pH value was 2.3-3.2, at which the content of Fe, Co and Ni in the deposit was 19.04 - 20.56%, 53.33 - 55.42% and 25.53 - 26.11%, respectively.

Fig.4(b) shows that Fe content in the deposit is 2.27-3.14 times Fe content in the bath, Co content is 2.17-2.9 times Co content in the bath and Ni content is 0.34-0.59 times Ni content in the bath, indicating that the change of pH value does not change the Fe-Co-Ni anomalous codeposition rule. However, this result presents a striking contrast to some researchers who thought that the anomalous behaviour was influenced by pH value [22-23]. When the pH value was 1.4 - 2.3, the deposition rate of Fe was close to that of Co. When the pH value was greater than 2.3, the deposition rate of Fe was significantly higher than that of Co. When the pH value was less than 3.2, the deposition rate of Ni remained almost unchanged, then slowly increased.

3.4. Influence of tartaric acid on Fe-Co- Ni alloy deposition

The standard electrode potential of Fe²⁺/Fe, Co²⁺/Co, Ni²⁺/Ni is -0.447V, -0.28V and -0.257V, respectively. Fe-Co-Ni alloy codeposition can be realized by adding tartaric acid as complexing agent in the electrolyte. Fig.5 shows the influence of tartaric acid on Fe-Co-Ni alloy codeposition at 3A/dm², 40⁰C and pH 2.3.

Fig.5(a) shows that when the concentration of tartaric acid in the electrolyte is 4-8 g/l, with the increase of tartaric acid concentration, the rate of Fe-Co-Ni alloy electrodeposition rises rapidly. When the tartaric acid concentration is 8 g/l, the deposition rate reaches a maximum value. Since then, with the further increase of tartaric acid concentration, the complexation of metal ions increases, resulting in the declining of codeposition rate.

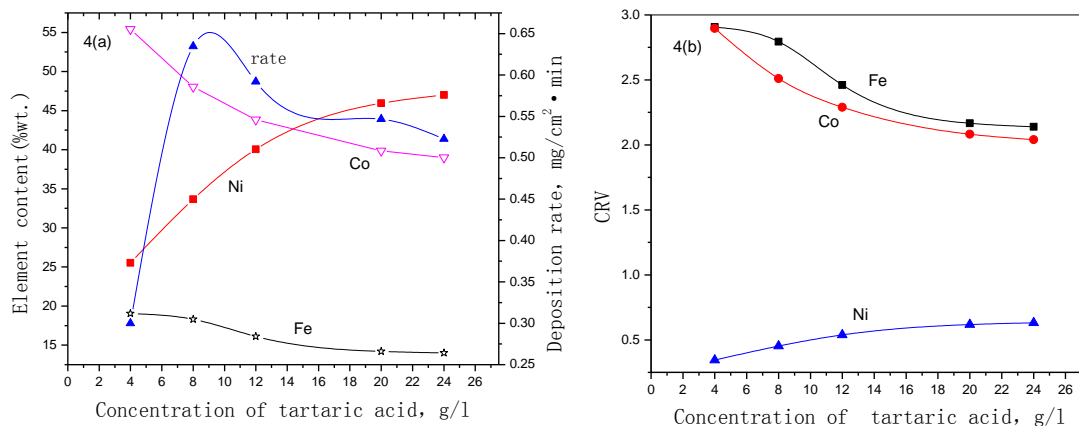


Figure 5. Influence of tartaric acid on Fe-Co-Ni alloy electrodeposition

With the increase of concentration of tartaric acid, the complexation of tartaric acid to metal ions is further enhanced, the polarization increases, and the concentration of free metal ion in the electrolyte reduces. Since Fe and Co preferentially deposit than Ni does, the increase of concentration of tartaric acid in the electrolyte will result in the decrease of Fe, Co content in the deposit, consequently the content of Ni increases. Experiments show that the concentration of tartaric acid of 8-12 g/l is appropriate. At this condition, silver white and bright Fe-Co-Ni deposits can be obtained with good toughness and compactness; the percentage of Fe, Co and Ni in the deposit was 19.04-16.12%, 55.42-43.84% and 25.53-40.05%, respectively. When the concentration of tartaric acid is greater, the brittleness of the deposit increases, and the performance degrades.

Fig.5 (b) shows that Fe content in the deposit is 2.14-2.91 times Fe content in the electrolyte, Co content is 2.04-2.9 times Co content in the bath, and the Ni content is 0.34-0.63 times Ni content in the bath. With the increase of tartaric acid concentration, the curve of Ni shows a rising trend, while the curves of Fe and Co show a downward trend, indicating that the deposition rate of Ni increases and the deposition rate of Fe and Co decreases. Nevertheless, the deposition rate of Fe is greater than that of Co, and Co is larger than that of Ni, the change of tartaric acid concentration does not affect the Fe-Co-Ni alloy anomalous codeposition behavior.

3.5. Influence of Co^{2+}/Ni^{2+} molar ratio on Fe-Co- Ni alloy deposition

Fig.6 shows the influence of Co^{2+}/Ni^{2+} molar ratio in the electrolyte on Fe-Co-Ni alloy codeposition at current density of 3 A/dm², temperature of 40 °C and pH of 2.3.

Fig.6(a) shows that with the increase of Co^{2+}/Ni^{2+} molar ratio in the electrolyte, the rate of Fe-Co-Ni alloy codeposition increases first and then decreases. When the ratio of Co^{2+}/Ni^{2+} is equal to 0.33, the deposition rate reaches a maximum value.

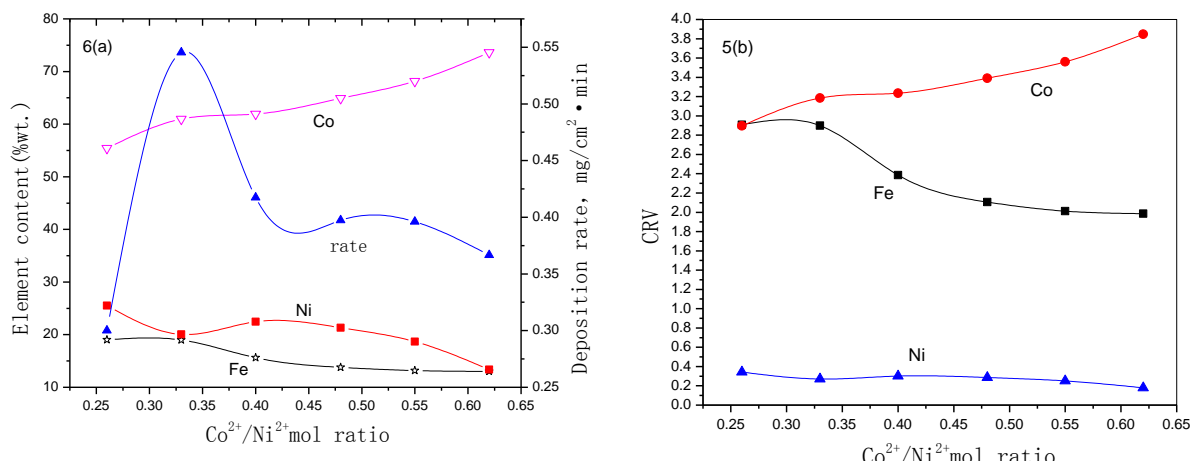


Figure 6. Influence of Co^{2+}/Ni^{2+} ratio on Fe-Co-Ni alloy electrodeposition

As the ratio of Co^{2+}/Ni^{2+} increases, Co content in the deposit increases gradually, while the content of Fe and Ni decrease. According to the literature [24], it can be inferred the reason is that the reduction potentials of Fe^{2+} and Ni^{2+} become more negative when increasing the Co^{2+}/Ni^{2+} ratio, which is not in favor of the increase of Fe and Ni amount in the deposit. The appropriate Co^{2+}/Ni^{2+} molar ratio is 0.26- 0.4, within this ratio range, the obtained Fe-Co-Ni alloy deposit is silver bright and smooth with good performance. The obtained deposits contain 19.04-15.62% of Fe, 55.42-61.93% of Co and 25.53-22.45% of Ni. Since then, with the further increase of Co^{2+}/Ni^{2+} molar ratio, the performance of the deposit declines with burr and dot on the edge.

Fig.6(b) shows that when Co^{2+}/Ni^{2+} molar ratio is 0.26 - 0.62, the content of Fe in the deposits is 1.99-2.91 times Fe in the electrolyte, the Co content is 2.9-3.85 times Co content in the electrolyte, and Ni content is 0.18 - 0.34 times Ni in the electrolyte. It can be seen that Fe and Co preferentially deposit than Ni. When the Co^{2+}/Ni^{2+} molar ratio is greater than 0.26, the curve of Co is located above the curve of Fe, the distance between curves of Co and Fe increases gradually, indicating that Co preferentially deposits than Fe. The deposition order of Fe and Co is related to Co^{2+}/Ni^{2+} molar ratio in the solution.

3.6. Performance, structure and surface morphology

The Fe-Co- Ni ternary alloy prepared at the above optimum conditions has good toughness with a glossy appearance of silvery white and bright smooth. The tensile strength of the deposit is up to 800 MPa, its elongation is 15% and the resistance is $75 \mu\Omega \cdot cm$.

Fig.7 is the EDS of Fe-Co-Ni ternary alloy. It can be seen from the figure that the weight percentage of Fe is 19.04%, Co is 55.42% and Ni is 25.53%, without sulfur, carbon and any other impurity elements in the deposit, indicating that the deposit is a pure ternary alloy of Fe-Co-Ni.

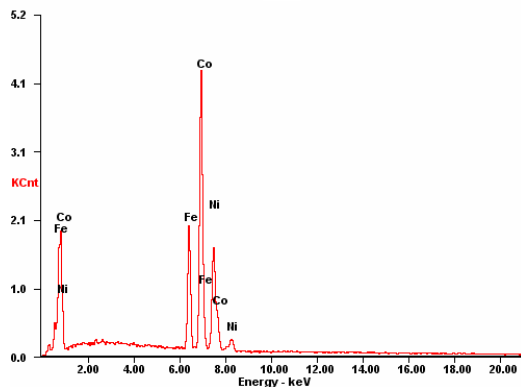


Figure 7. EDS pattern of Fe-Co-Ni alloy

Fig.8 is the XRD diagram of Fe-Co-Ni alloy deposit with 19.04% Fe, 55.42% Co and 25.53% Ni. Through the analysis of the PDF card, it can be seen that Fe-Co-Ni alloy deposit is a solid solution with a body centered cubic structure. Its crystal lattice constant is 2.88Å, containing FeCo and Fe19Ni phases. Among them, FeCo phase has clear, sharp diffraction peaks at 2θ of near 45.168 °, 65.792 ° and 83.392 °, their crystal plane index is (110), (200) and (211), respectively. Fe19Ni phase has two low diffraction peaks at 2θ of near 44.489 ° and 64.737 ° with the crystal plane index of (110) and (200).

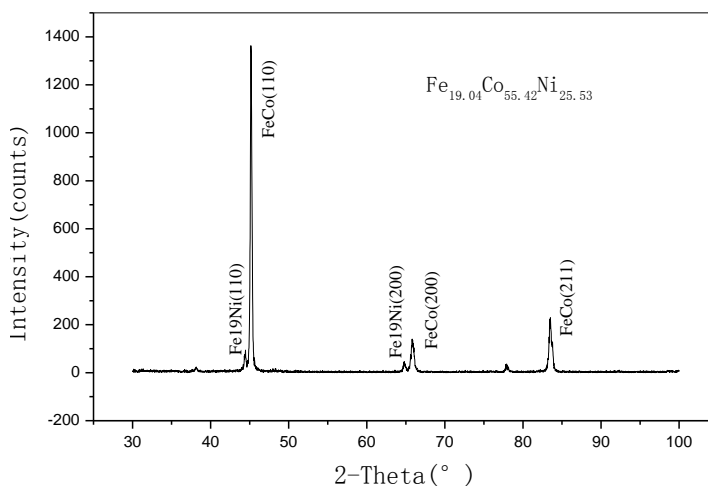


Figure 8. XRD pattern for the Fe-Co-Ni alloy deposit

Fig.9 is the SEM diagrams of Fe-Co-Ni alloys with compositions of Fe₁₈Co₄₉Ni₃₃ and Fe₁₇Co₅₂Ni₃₁. Both of the deposits are bright and smooth with no microcracks on the surface, indicating low residual stress. The spherical grains of Fe₁₈Co₄₉Ni₃₃ are uniform, fine and compact, and the grain boundary is clearly visible. With increase of Co content, the deposit of Fe₁₇Co₅₂Ni₃₁ gets more and more bright and smoothly, its grains are small and could not be identified clearly.

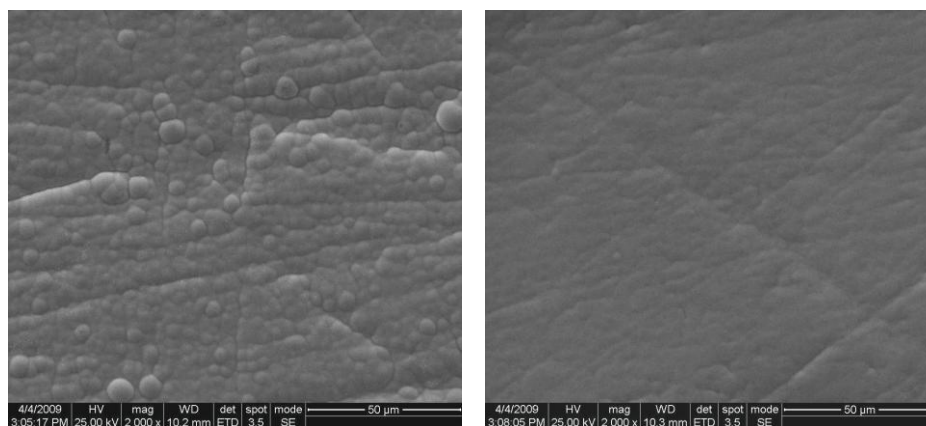


Figure 9. SEM micrographs of the Fe-Co-Ni deposit of $\text{Fe}_{18}\text{Co}_{49}\text{Ni}_{33}$ and $\text{Fe}_{17}\text{Co}_{52}\text{Ni}_{31}$

4. CONCLUSION

1. The rate of Fe-Co-Ni alloy electrodeposition increased with the increase of current density, temperature, and pH value. It increased first and then decreased with the increase of tartaric acid concentration and the $\text{Co}^{2+}/\text{Ni}^{2+}$ mole ratio.

2. Fe content in the deposit increased first and then decreased with the increase of current density and pH value, and decreased with the increase of temperature, tartaric acid concentration and $\text{Co}^{2+}/\text{Ni}^{2+}$ ratio. Co content in the deposit increased first and then decreased with the increase of current density and temperature, decreased with the increase of pH value and the tartaric acid concentration, and increased with increasing the $\text{Co}^{2+}/\text{Ni}^{2+}$ mole ratio. Ni content in the deposit decreased first and then increased with increase of current density, increased with increase of temperature, pH value and the tartaric acid concentration, and decreased with increase of $\text{Co}^{2+}/\text{Ni}^{2+}$ mole ratio.

3. The optimum conditions were current density of 4 A/dm^2 , temperature of $40 \text{ }^\circ\text{C}$, pH of 2.3-3.2, tartaric acid concentration of 8 -12 g/l, $\text{Co}^{2+}/\text{Ni}^{2+}$ molar ratio of 0.26-0.4.

4. Fe-Co-Ni alloy electrodeposition is anomalous. Fe preferentially deposits than Co, Co preferentially deposits than Ni. The characteristics of anomalous codeposition do not change with the changes of current density, pH value and tartaric acid concentration. When the temperature is higher than $60 \text{ }^\circ\text{C}$ and $\text{Co}^{2+}/\text{Ni}^{2+}$ mole ratio is greater than 0.26, Co deposits preferentially than Fe.

5. Fe-Co-Ni alloy obtained at optimal conditions is bright, smooth, a solid solution with good toughness and a body centered cubic structure.

References

1. H.G. Zheng, J.H. Zeng, J.H. Liang, *Acta Metall. Sinica.*, 35 (8) (1999) 837.
2. X.Y. Kong, J.S. Wu, *J. Funct. Mate.*, 31(5) (2000) 479.
3. T. Osaka, *Electrochim. Acta*, 45 (2000) 3311.
4. T. Osaka, M. Taka, *Nature*, 392 (1998) 796.

5. T. Pikula, L. Kubalova, D. Oleszak, *J Alloy Compd.*, 483(2009) 582.
6. X.G. Li, F.H. Liao, *Chin. J. Process Eng.*, 2(4) (2002) 295.
7. Saedi, M. Ghorbani, *Mater. Chem. Phys.*, 91 (2005) 417.
8. V.B. Singh, P.K. Tikoo, *Electrochim. Acta*, 22 (10) (1977) 1201.
9. Y. Omata, *Magn. Jpn.*, 5 (1) (1990) 17.
10. X.M Liu, J.O.Rantschler, C.Alexander, G.Zangari, *Magnetics*, 39 (5) (2003) 2362.
11. H. J Zheng, C.N Ma, J.G Huang, R.Q. Zhang, Y.J Chen, *Mater. Prot.*, 37 (6) (2004) 17.
12. J.F Li, Z. Zhang, J.Y. Yin, G.H. Yu, C. Cai, J.Q Zhang, *Trans. Nonferrous Met. Soc. China*, 16(2006) 659.
13. W.X Xu, Z.M Qian, *Physi. Exam. Test.*, 25 (3) (2007) 19.
14. Attila Csik, Kálmán Vad, Enikő Tóth-Kádár, László Péter, *Electrochem. Commun.*, 11(6) (2009) 1289.
15. A. Bai, C.C. Hu. *Electrochem. Commun.*, 5 (1) (2003) 78.
16. A. Bai, C.C.Hu, T.C.Wen, *Electrochim. Acta*, 48 (2003) 2425.
17. Brenner, *Electrodeposition of Alloys, Principles and Practice*, Chapter 30, Academic Press, New York, 1963, p. 194.
18. H. Dahms, I.M. Croll, *J. Electrochem. Soc.* 112 (1965) 771.
19. K. Higashi, K. Higashi, H. Fukushima, T. Urakawa, T. Adaniya, K. Matsudo, *J. Electrochem. Soc.* 128 (1981) 2081.
20. R. Fratesi, G. Roventi, G. Giuliani, C.R. Tomachuk, *J. Appl. Electrochem.* 27 (1997) 1088.
21. J.Y. Fei, G.D. Wilcox, *Electrochim. Acta*, 50 (2005) 2693.
22. E.I. Cooper et al., *IBM. J. Res. Develop.* 49 (2005) 103.
23. S. Hessami, C.W. Tobias, *J. Electrochem. Soc.* 136 (1989) 4611.
24. C.Z. Yao, P. Zhang, M. Liu, G. R. Li, J.Q. Ye, P. Liu, Y. X. Tong, *Electrochimica Acta*, 53 (2008) 8362